Sleep-insomnia superposition: opposing brain signatures of sleep in task-based and resting-state conditions

Mohamed Abdelhack[1], Peter Zhukovsky[2,3], Milos Milic[1], Shreyas Harita[1,5], John Griffiths[1,2,4,5], Sean L Hill[1,2,4,5,7], Daniel Felsky*[1,4,5,6]

[1] Krembil Centre for Neuroinformatics, Centre for Addiction and Mental Health, Toronto, ON, Canada
[2] Campbell Family Mental Health Research Institute, Centre for Addiction and Mental Health, Toronto, ON, Canada
[3] Centre for Depression, Anxiety and Stress Research, McLean Hospital, Boston, MA
[4] Department of Psychiatry, Temerty Faculty of Medicine, University of Toronto, Toronto, ON, Canada
[5] Institute of Medical Science, University of Toronto, Toronto, ON, Canada
[6] Department of Biostatistics, Dalla Lana School of Public Health, University of Toronto, Toronto, ON, Canada
[7] Vector Institute for Artificial Intelligence, Toronto, Canada

*Corresponding author
Daniel Felsky PhD
Independent Scientist, Krembil Centre for Neuroinformatics, Centre for Addiction and Mental Health
Assistant Professor, Department of Psychiatry and Dalla Lana School of Public Health, University of Toronto
12th Floor, 250 College Street, Toronto ON, M5T 1R8, Canada
Daniel.felsky@camh.ca; dfelsky@gmail.com
www.felskylab.com
(416) 535 8501 x33587

Abstract

Sleep and mental health have complex relationships, with sleep-associated alterations in brain dynamics and structure impacting a range of symptoms and cognitive abilities. We analyzed the correlations between task and resting-state brain-wide signatures of sleep, cognition, and depression in over 30,000 individuals. Insomnia and depression correlated negatively with sleep duration at task condition, but positively at resting-state with an associated hyperconnectivity disputing conventional assumptions and suggesting hyperarousal-insomnia link.

Main

The relationships between sleep, neurocognitive processes, and depression are complex and fraught with paradoxical relationships. Depressive symptoms are linked to both increases[1] and decreases[2] in sleep, and acute sleep deprivation showed antidepressant effects[3]. Neural correlates of sleep are also linked to both hyper and hypo-activation in different task environments[4,5], and both undersleeping and oversleeping result in cognitive decline[6]. The majority of our current understanding of sleep has come from acute sleep deprivation experiments and clinical sleep disorders which cover only fringe conditions in comparison with the general population[2,4,5,7]. Insomnia, daytime dozing, and low sleep quality have been associated with aberrant functional connectivity in many brain regions[4]; however, most neuroimaging studies have been underpowered, yielding heterogeneous results and inconclusive evidence. This has produced a gap in our understanding on the role of sleep in mental and cognitive health as well as how sleep affects the brain under different conditions and cognitive loads.

Some initial attempts toward decoding these complex relationships at the population level have been made[8]. Studies using UK Biobank (UKB)[9] and the Human Connectome Project (HCP)[10] data have found links between poor sleep and depressive symptoms mediated by functional connectivity[11]. A systematic analysis of multiple sleep phenotypes and brain data in UKB[12] identified resting-state brain activation as a predictor of insomnia and daytime dozing with almost no significant associations with task-based fMRI features. Crucially, these studies were limited to self-reported sleep measures and did not investigate the relationships between different neural signatures of tested phenotypes.

To address these gaps, we perform a multi-step analysis of two independent cohorts and examine summary statistics from previously published analyses through a new lens. First, we map the associations of sleep quality - measured subjectively by self-report and objectively by accelerometry - with both task-based and resting-state measures of brain function in the UKB and HCP. We then tested the correlations between the resulting maps of sleep with those for cognitive performance and depressive symptoms, finding seemingly contradictory patterns of resting-state and task-based activation in response to poor sleep.

We first constructed brain maps of each phenotype using task-based and resting-state fMRI (**Figure 1BC**). For the task data, we fit multivariate models[13,14] to classify face and shape trials. We used classification accuracies from each region as a proxy for its cortical coding in response to stimuli (See Online Methods and Extended Results; **Figure S3**). For resting-state data, we used the functional connectivity measures between independent components (see Online Methods). We then measured the association of classification accuracy and functional connectivity data with five behavioral measures: sleep quality measured by an accelerometer (duration of longest sleep bout), self-reported insomnia frequency, self-reported daytime dozing frequency, cognitive ability measured by a symbol-digit-substitution task[15], and subclinical depression symptoms measured by PHQ-2 score[16] (See Online Methods).

We then calculated pairwise correlations between the brain maps of the five phenotypes in task and resting data in comparison to the phenotypic partial correlation **(Figure 1B)**. Phenotypic correlations showed small effect sizes, with accelerometer-measured sleep quality negatively correlated with depression (r=-0.038; p=1.04×10^{-4}), insomnia (r=-0.072; p=2.21×10^{-15}) and daytime dozing (r=-0.11; p=1.29×10^{-35}). Depressive symptoms positively correlated with self-reported insomnia (r=0.15; p=5.64×10^{-63}). For the task-based condition, in directional agreement with our observed phenotypic correlations, accelerometer-measured duration of longest sleep bout negatively correlated with depression (r=-0.63; p=5.07×10^{-21}), insomnia (r=-0.14; p=0.04), and daytime dozing (r=-0.64; p=1.00×10^{-21}). Depressive symptoms correlated positively with insomnia (r=0.17; p=0.03) indicating similar effects across the cortex. Maps from anatomical cortical thickness maps showed consistent results (Extended Results; **Figure S9**).

In the resting-state condition, a notable difference emerged. In contrast to the results from the task condition and from phenotypic correlations, there were nontrivial positive correlations between the neural signature for duration of longest sleep bout and those for both self-reported insomnia (r=0.59; p=2.71×10^{-21}) and depressive symptoms (r=0.48; p=1.87×10^{-13}). This indicated a similarity between the functional connectivity changes associated with longer continuous sleep, higher frequency of insomnia, and depressive symptoms frequency which is counterintuitive. To confirm this finding, we analyzed independently modeled imaging associations with self-reported insomnia, daytime dozing, and sleep duration published by Fan et al.[12] (**Table 4**) and performed additional analyses in 807 participants from the HCP dataset with proxy phenotypes (see Online Methods). Both analyses were in agreement with our findings (**Figure S4**).

To shed light on this counterintuitive but durable observation, we tested a hypothesis that resting-state neural patterns of individuals with insomnia and depression resemble a long-sleep-like hyperattentive state, preventing them from sleeping. We stratified study participants into approximately equal groups split by the duration of longest sleep bout median value (short-sleepers: <6.8 hours; long-sleepers: ≥6.8; **Figure 1C**). The positive correlation between sleep duration and both self-reported insomnia and depressive symptoms persisted only within the long-sleepers (insomnia: r=0.73; p=4.41×10^{-36}; PHQ-2: r=0.59; p=3.34×10^{-21}). In the short-sleeper group, we observed no significant correlation between neural signatures of sleep duration and that for PHQ-2 (r=-0.079; p=0.26), and found a significant negative correlation of sleep duration with self-reported insomnia (r=-0.20; p=0.003). The insomnia-sleep pattern was interestingly also reproduced in stratified phenotypic correlation (**Figure S2**). We also tested a hypothesis where higher levels of depressive symptoms drive the discrepancy and split by depression score[16] but the pattern persisted in not-depressed group which could be due to the imbalance where the depressed group only had 944 participants (**Figure S5**). Results indicate that the resting-state signal of insomnia and depression resembles that of a rested wakefulness state, which in turn could prevent from falling asleep and maintain a hyperarousal state[2,17–19]. It also suggests that the relation with insomnia is non-linear where insomnia also correlates with short continuous sleep.

In order to investigate the directionality of associations of the neural connectivity patterns giving rise to this discrepancy, we compared global connectivity across resting and task conditions. We calculated the representational connectivity for the task condition and seed-based connectivity for resting condition (see Online Methods). We modeled associations with our five phenotypes across all connectivity and aggregate brain-wide average connectivity (**Figure 2A,C**). We also modeled the association of the network-specific average connectivity (**Figure 2B**) in order to investigate intra- and inter-network connectivity changes. The task condition showed a predominantly negative association between connectivity and depression and insomnia (**Figure 2A**) suggesting hypoconnectivity associated with these phenotypes. However, in the resting condition, the associations were mostly positive, suggesting hyperconnectivity. This hyperconnectivity could reflect difficulty in falling asleep where effective connectivity breaks down[20]. Network-wise connectivity associations for task condition were global across networks while resting was largely inverted in visual and somatomotor networks (**Figure 2B**).

We then investigated the functional associations of the phenotypes of interest (**Figure 3**). Measured sleep, depression, and cognition showed significant associations predominantly across intermediate visual and multimodal parietal regions (**Figure 3B, S6**). Longer sleep bouts were associated with a higher decoding accuracy primarily in lateral occipital regions (**Figure 3B**) which are intermediate visual processing areas. This was accompanied by a significant resting-state connectivity association between IC5 and IC18 (**Figure 3C**). Seed-based connectivity analysis showed a similar association between the posterior-inferior frontal junction (IFJp) and almost all the occipital regions belonging to IC18 (**Figure 3D**). Taken together, these results point to an association of sleep duration with the top-down attentional regions projecting to intermediate visual cortex. More resting-state associations were found for other phenotypes (Extended Results; **Figure S6–8**).

Our study is limited by its focus on a general population cohort, not describing clinical populations, and relying mainly on self-reported measures. In addition, task-based signatures of cognition were not entirely consistent between UKB and HCP possibly due to a difference in the cognitive measure used[21]. Similarly, task-based fMRI results might not necessarily generalize to other tasks, limiting the conclusions of this analysis. However, the alignment with phenotypic results suggests that it would. Also, to maximize the number of participants and strengthen statistical power in the association analyses, we included all participants with an available measurement for each phenotype independently (**Figure S1**). This led to different numbers of participants in the models of each phenotype (**Table 2**).

We counterintuitively found similarities in resting-state neural signatures among people with insomnia, long sleep, and depression symptoms which could signal hyperarousal in resting state activity. This hyperarousal could increase the possibility of cognitive fatigue that may lead to a reduction in task-based activation[17,19]. This persistent fatigue could give rise to depressive symptoms with daytime dozing acting as a compensatory mechanism, and may partly explain the success of sleep deprivation as a therapy for depression[3]. It also highlights the heterogeneity of sleep quality factors where different components could have varying neural signatures. We uncover a phenomenon of brain-wide similarities between sleep quality,

insomnia, and depressive symptoms that could help guide advancing clinical practices to investigate more fine-grained details of sleep habits to design the optimal care plans all while concurrently tracking the cognitive load of patients.

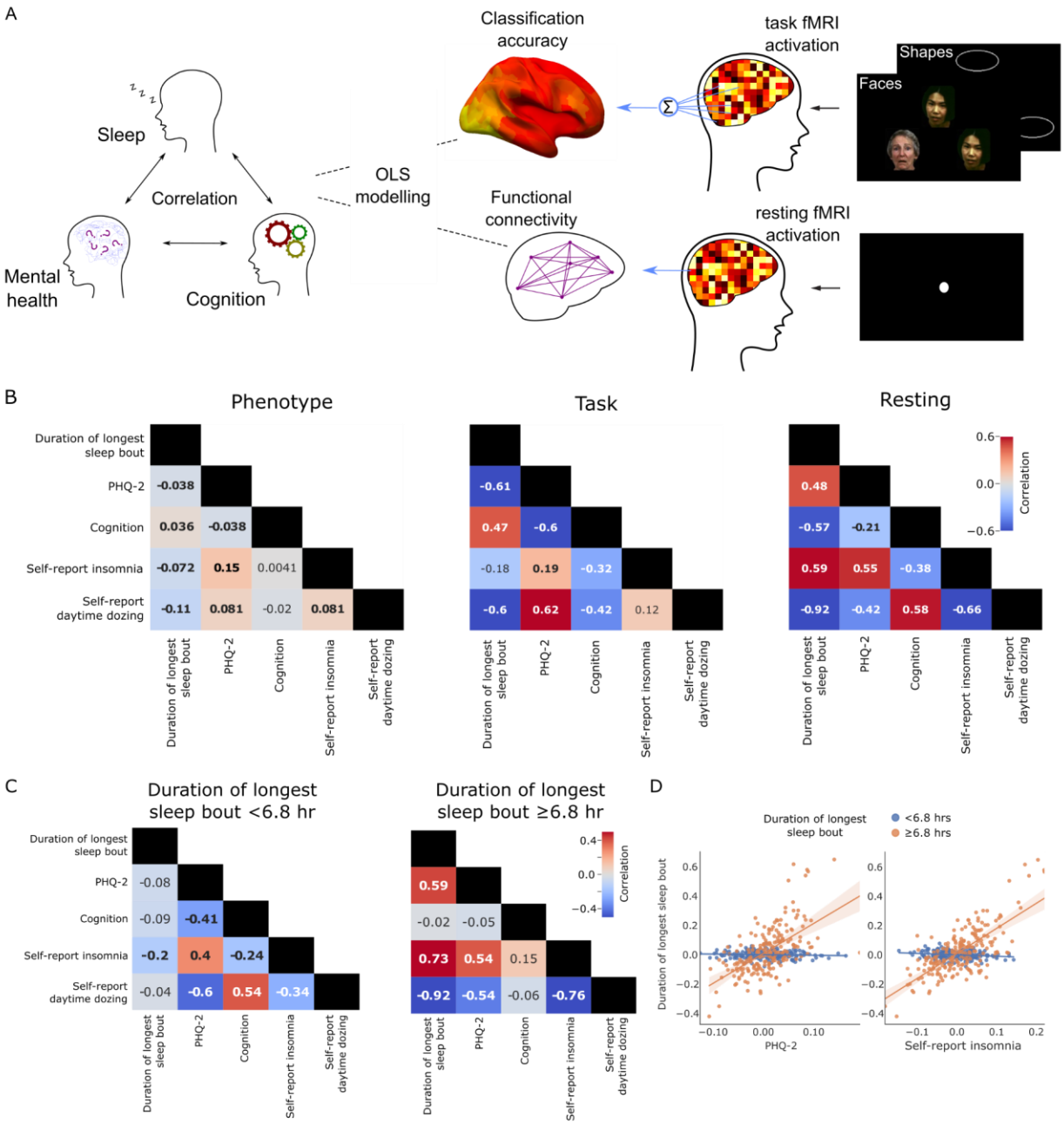

Figure 1: Data analysis protocol diagram and intercorrelation between tested phenotypes. **A** shows the fMRI analysis, multivariate pattern analysis for task and functional connectivity analysis for resting were conducted and the subsequent linear modelling of the classification accuracy with the phenotypes to build a cortical map of associations (stimulus images obtained by permission from Prof. Deanna Barch). Later the intercorrelation analysis of these variables are calculated for phenotypes and neural association maps. **B** shows the partial correlation map between the tested phenotypes of sleep (duration of longest sleep bout, self-reported insomnia, and self-reported daytime dozing), depression symptoms (PHQ-2 score), and cognition (bolded numbers are correlations significantly different from zero) and pairwise correlation of task and resting-state brain-wide associations. **C** shows the pairwise correlation values for the

coefficients of the models split by the duration of longest sleep bout. Bolded values are statistically significant. **D** shows a scatter plot with the line of fit between the coefficients of the models for two pairs of phenotypes (duration of longest sleep bout and PHQ-2; duration of longest sleep bout and self-reported insomnia).

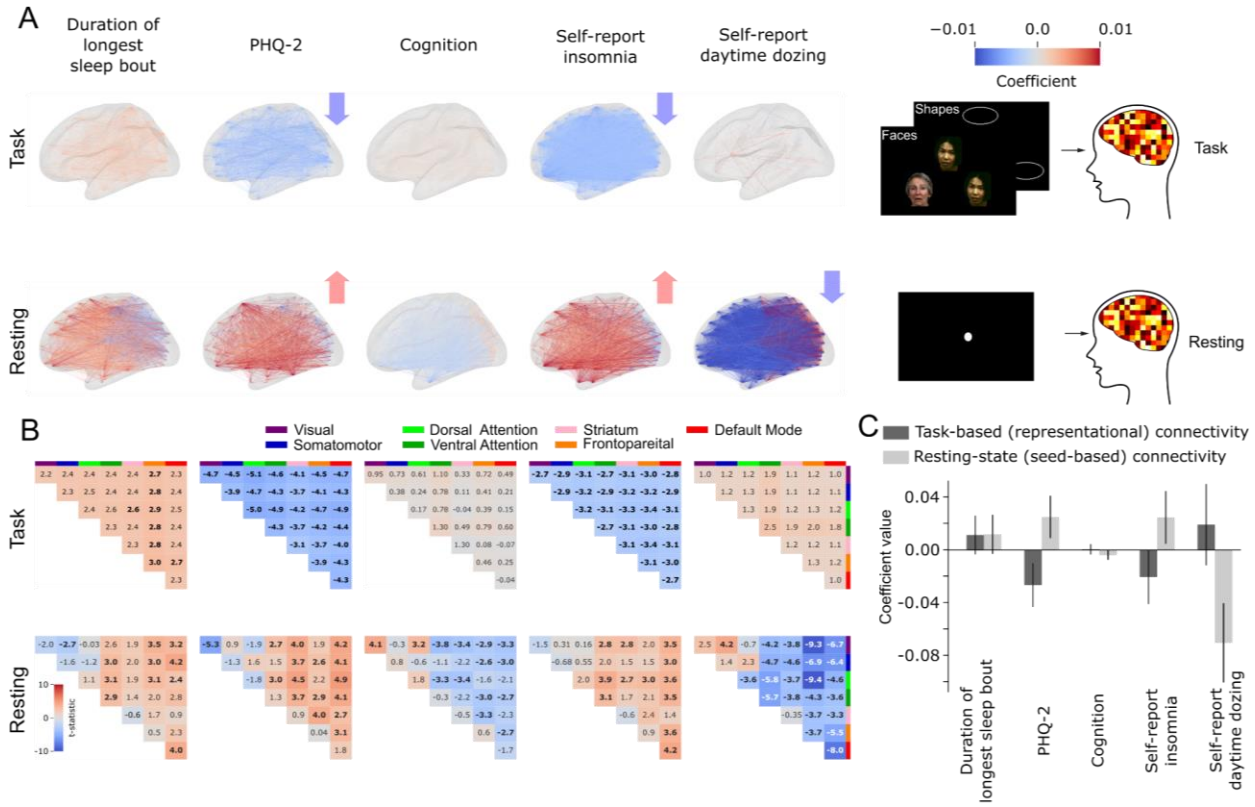

Figure 2: Brain regions are hyperconnected with PHQ-2 and insomnia in resting condition but hypoconnected in task condition. **A** shows the significant brain representational and functional connectivity associations with the five phenotypes for each connection between HCP180 regions. **B** Network-wise representational (upper) and functional (lower) connectivity associations (model t-statistic) with the different phenotypes. Bolded associations are statistically significant. **C** Global mean connectivity associations with the five phenotypes. Error bars represent 95% confidence intervals after correcting for multiple comparisons over 5 measures.

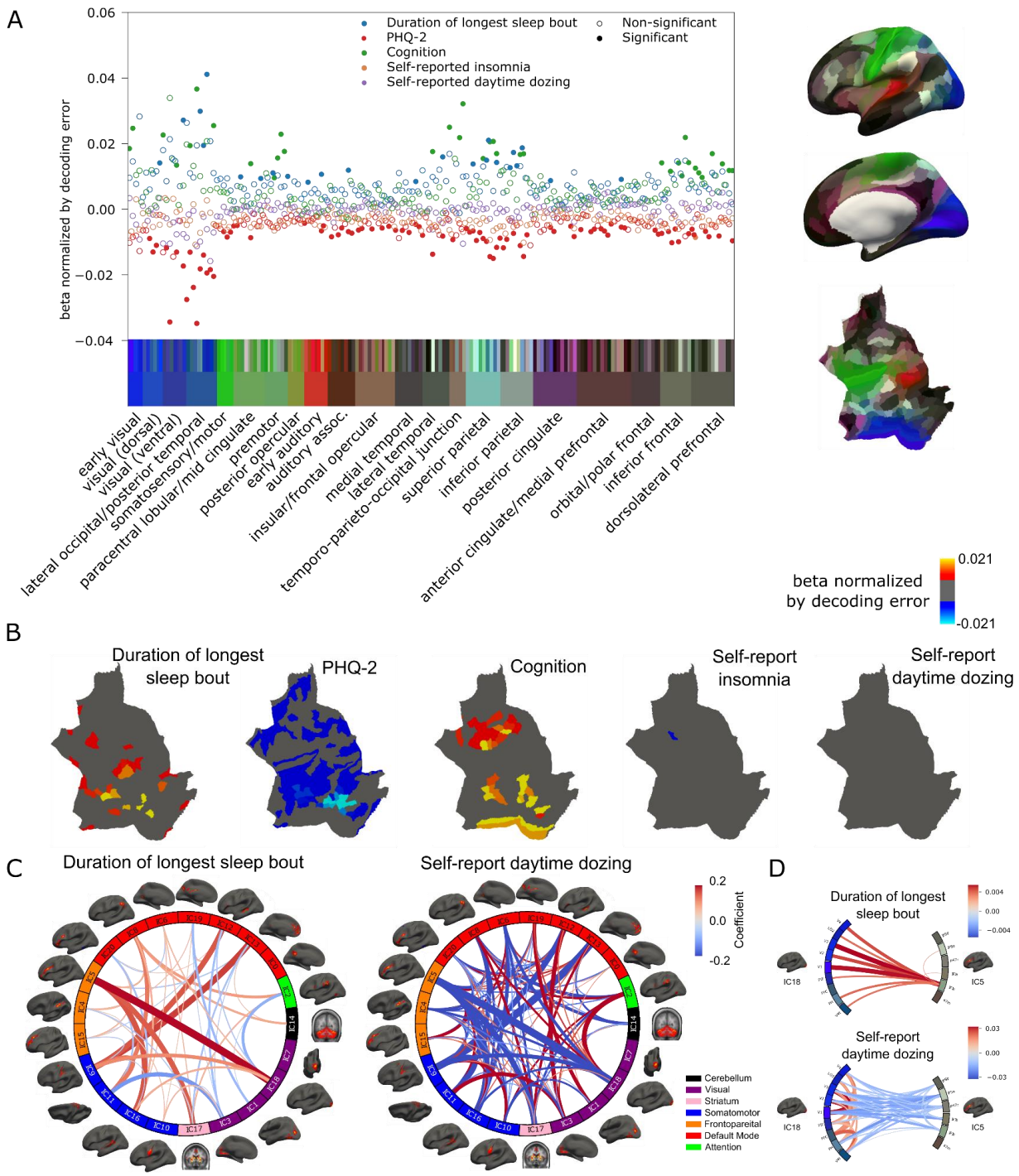

Figure 3: Results of the associations from the task-based fMRI data. A summarizes the overall beta values of the models normalized by decoding accuracy. The regions are organized and color coded according to their groupings in the human connectome project[22] where the region color maps are shown on the right. **B** shows the brain region maps with significant associations color coded by the beta values normalized by decoding accuracy for each of the phenotype models. **C** shows the functional connectivity associations for the accelerometer-

measured duration of longest sleep bout and self-reported daytime dozing. The different components are grouped and color-coded based on the Yeo 7 Networks[23]. **D** zooms in on the associations between IC5 and IC18 showing seed-based correlation associations between different regions belonging to the components of interest.

References

1. Singh, T. & Williams, K. *Psychiatry Edgmont* **3**, 33–39 (2006).
2. Baglioni, C., Spiegelhalder, K., Lombardo, C. & Riemann, D. *Sleep Med. Rev.* **14**, 227–238 (2010).
3. Boland, E.M. et al. *J. Clin. Psychiatry* **78**, 893 (2017).
4. Fasiello, E. et al. *Sleep Med. Rev.* **61**, 101569 (2022).
5. Krause, A.J. et al. *Nat. Rev. Neurosci.* **18**, 404–418 (2017).
6. Tai, X.Y., Chen, C., Manohar, S. & Husain, M. *Commun. Biol.* **5**, 1–10 (2022).
7. Fortier-Brochu, É., Beaulieu-Bonneau, S., Ivers, H. & Morin, C.M. *Sleep Med. Rev.* **16**, 83–94 (2012).
8. Yu, J. et al. *Sleep Med.* **103**, 41–50 (2023).
9. Miller, K.L. et al. *Nat. Neurosci.* **19**, 1523–1536 (2016).
10. Van Essen, D.C. et al. *NeuroImage* **62**, 2222–2231 (2012).
11. Cheng, W., Rolls, E.T., Ruan, H. & Feng, J. *JAMA Psychiatry* **75**, 1052–1061 (2018).
12. Fan, Z. et al.2022.09.08.22279719 (2022).doi:10.1101/2022.09.08.22279719
13. Haxby, J.V. et al. *Science* **293**, 2425–2430 (2001).
14. Kamitani, Y. & Tong, F. *Nat. Neurosci.* **8**, 679–685 (2005).
15. Jaeger, J. *J. Clin. Psychopharmacol.* **38**, 513–519 (2018).
16. Kroenke, K., Spitzer, R.L. & Williams, J.B.W. *Med. Care* **41**, 1284–1292 (2003).
17. Bonnet, M.H. & Arand, D.L. *Sleep Med. Rev.* **14**, 9–15 (2010).
18. Fernández-Mendoza, J. et al. *Psychosom. Med.* **72**, 397–403 (2010).
19. Riemann, D. et al. *Sleep Med. Rev.* **14**, 19–31 (2010).
20. Massimini, M. et al. *Science* **309**, 2228–2232 (2005).
21. Hsu, W.-C. et al. *Medicine (Baltimore)* **95**, e4535 (2016).
22. Glasser, M.F. et al. *Nature* **536**, 171–178 (2016).
23. Thomas Yeo, B.T. et al. *J. Neurophysiol.* **106**, 1125–1165 (2011).

Online Methods

Software

We utilized FreeSurfer and FSL tools for brain region parcellation and label transformation as well as for cortical thickness measurements and seed-based correlation analysis and higher-level modeling of its results. We used python 3.6 for subsequent analyses with Brain Decoder Toolbox 2 for brain region data extraction, scikit-learn for SVM classifier construction, statsmodels for OLS model creation. For plotting and visualization, we used the libraries seaborn [1] and mne-connectivity.

Dataset

Data was obtained from UK Biobank [2,3] application #61530. We collected data for the functional magnetic resonance imaging for the resting state and task-based paradigms as well as the anatomical data (N=30,945). We also utilized the task data from E-Prime software (software data) to characterize the task-based runs. For sleep data, we obtained both data from the self-report sleep quality measures collected at the same imaging instance and the measured sleep data from the accelerometry data [4]. Other psychiatric (PHQ-2) and cognitive measures (symbol digit substitution task) were collected from the self-reported mental health questionnaires and cognitive test results [5] conducted at the same imaging instance. **Table S1** indicates the variable codes from UK Biobank and the number of valid subjects extracted for each data modality. Covariates were extracted from the demographics data in UK Biobank (sex, age, socioeconomic status, ethnicity, and education level), and the measurement-specific factors (difference in time between accelerometry measurement and brain image acquisition, head motion, face-shape task performance, and measurement site).

Phenotypic correlation analysis

We measured the pairwise phenotypic partial correlations between five output parameters: sleep quality measured by an accelerometer (duration of longest sleep bout), self-reported sleeplessness/insomnia frequency, self-reported daytime dozing frequency, cognitive ability measured by number of correct matches in a symbol-digit substitution task[5], and subclinical depression score measured by the PHQ-2 scale[6] with age, sex, study site, ethnicity, socioeconomic status, difference between time of accelerometer measurement and assessment center visit (only for the accelerometer output parameter), and education level as covariates. We calculated confidence intervals and significance using the 99% confidence intervals to correct for multiple comparisons (0.05 significance level over five outputs).

ROI-based analysis

Regions of interest for the multivariate pattern analyses were constructed using the predefined cortical parcellations from the Human Connectome Project (HCP)[7]. We combined the bilateral regions of interest resulting in 180 parcellations. The labels from the HCP parcellation were transformed using FreeSurfer software[8] from the fsaverage subject cortical surface to each subject's surface in the dataset. Labels were then transformed into the volume space of the fMRI data for each of the resting state and task-based paradigms.

Task fMRI analysis

The task fMRI experiment in UK Biobank data comprised a modified version of the face-shape matching task[9,10]. In this task subjects viewed a central cue stimulus accompanied by two stimuli on the right and the left with one of them matching the central cue. Subjects were tasked to press a button identifying which of the two stimuli is the one matching the central cue. The trials contained either human faces or 2D shapes (circle, horizontal ellipse, and vertical ellipse). In order to perform brain-wide association analysis with the task-based fMRI data, we built multivariate classification models[11,12] using support vector machines (SVM) to classify the face and shape trials regardless of subject's performance. Models were created for each region of interest where regions were delineated according to the human connectome project (HCP) parcellation[10]. We carried forward the classification accuracies from each region as a proxy for its cortical activation in response to the visual stimuli. We then measured the association of classification accuracy with our phenotypes of interest using ordinary least squares (OLS) regression models. We created ordinary least square models relating the classification accuracy of each region and sleep efficiency. We also added the relevant covariates to the model (sex, age, imaging site, head motion, socioeconomic status, education level, ethnicity, task performance accuracy mean, task response time mean, task response time standard deviation, sex and age interaction, and accelerometry time relative to brain acquisition). To correct for multiple comparisons, we adjusted the p-values for the false discovery rate using the Benjamini/Hochberg method. We also divided the resulting model coefficients by the classification error to up-weight regions with voxels most responsive to the stimuli.

Multivariate pattern analysis

We utilized the readily preprocessed task-based fMRI data from UK Biobank to create classifiers between faces and shapes for each brain region. Time series from each region was extracted using Brain Decoder Toolbox 2 for Python (https://github.com/KamitaniLab/bdpy). We then applied further preprocessing to the data where the data volumes were shifted by 5 volumes (3.675 seconds) to compensate for the hemodynamic delay. Data was then filtered to remove the slow signal shift along the run, and then samples were normalized by the mean value to extract the percent signal change. We then averaged the samples belonging to the same classification category within each block to improve the signal-to-noise ratio. Finally, the data points without stimulus were removed and the samples were then randomized. We ended up with 60 data points for the classifier which were then randomized and divided into training and test datasets in a 6-fold cross-validation scheme. For each fold, we trained a binary support vector machine classifier with a linear kernel to classify the faces and shapes. The mean classification accuracy from each region was then calculated and utilized as a proxy for the strength of encoding of stimuli in this brain region.

Representational connectivity analysis

We extracted and preprocessed the task fMRI data in a similar fashion as in the MVPA analysis. We then divided the stimuli into 7 different categories based on the content of stimuli with three categories representing shapes (circle, horizontal ellipse, and vertical ellipse) and four representing faces (male, female, angry, and fearful faces). The voxel data for each of these conditions were then averaged creating a vector of voxel data for each region. We then computed the representational dissimilarity matrix (RDM)[13] for each region. To calculate representational connectivity, we conducted a second-order correlation analysis between region pairs by calculating the Pearson correlation coefficient between the lower triangles of their RDMs.

Cortical thickness measurement

Cortical thickness was measured for each brain region using Freesurfer software anatomical statistics measurement tools using the FreeSurfer reconstructed brain anatomy images provided by UK Biobank. We then created ordinary least squares models relating cortical thickness data to sleep efficiency and relevant covariates (sex, age, socioeconomic status, education level, ethnicity, imaging site, sex and age interaction, accelerometry time relative to brain acquisition). To correct for multiple comparison, we adjusted the *p*-values for false discovery rate using the Benjamini/Hochberg method.

Functional connectivity analysis

We extracted the readily-processed functional connectivity data based on full correlation from UK Biobank repository (variable code: 25750) and created ordinary least square models relating functional connectivity between each node (independent component) and the five phenotypes. We also added the relevant covariates to the model (sex, age, imaging site, head motion, socioeconomic status, education level, ethnicity, sex and age interaction, and accelerometry time relative to brain acquisition). To correct for multiple comparisons, we adjusted the *p*-values for multiple comparison using Bonferroni's correction for five phenotypes and 21 independent components.

Seed-based correlation analysis

In order to create more fine-grained connectivity patterns that also map to the same regions as the task-based fMRI, we ran a seed-based correlation analysis on each region using FSL dual regression tool[14]. We then divided the resulting correlation map into the HCP region space computing the mean over each region resulting in a 180 x 180 matrix of connectivity. We then normalized the rows of the matrix by the self-correlation values (diagonal of the matrix). Results were used to construct a higher-level model with sleep efficiency as the independent variable and the resting state covariates similar to the OLS models previously described in the functional connectivity analysis.

Brain-wide mean connectivity analysis

We calculated brain-wide mean connectivity by averaging the seed-based connectivity across all node pairs from the HCP regions for the resting state data. For the task-based data we averaged the representational connectivity measures across all the regions. We then built OLS models for each mean connectivity value for each phenotype and calculated the model coefficients and confidence intervals based on a *p*-value of 0.01 based on Bonferroni correction for five phenotypes.

Human connectome project data analysis

We extracted the HCP data from the young adult project[15,16]. We extracted the data for the emotion task and the resting-state. For the emotion task, there were two runs for each subject with the exact same task as that for UK Biobank. We concatenated the data for these two runs and constructed the SVM models similar to the protocol used for UK Biobank. For the resting-state data, we utilized the already processed functional connectivity based on the full correlation between nodes defined by the group-ICA analysis.
For the phenotypes equivalent to those we analysed in the UK Biobank, we used the sleep parameters based on the PSQI sleep score[17] as there was no objective sleep measures. We utilized the self-reported sleep duration as a proxy for the accelerometer-measured duration of longest sleep bout, the PSQI second component that relies on difficulty of falling asleep as a proxy for insomnia, and the answer to the question on trouble staying awake during daytime activities as a proxy for daytime dozing. For depression measure, we used the reported sadness score from the assessment of self-reported negative affect measure from the NIH toolbox[18]. For cognition, despite the HCP data containing cognitive test, the test score we utilized for the UK Biobank was not done for the HCP cohort. We utilized the Mini-Mental State Examination results as generic test for cognition[19]. The complete set of subjects with all imaging and behavioral phenotypes available was 807. We included covariates representing age, sex, study site, ethnicity, socioeconomic status, and education level to the OLS models.

Acknowledgements
The authors would like to thank the members of the Whole Person and Population Modelling group members for the valuable support, discussions, and feedback throughout the different stages of this study. We also thank Qing Chang for his help with data access and Prof. Colin Hawko and Dr. Erin Dickie for their helpful discussions over fMRI data processing methodology. We would also like to thank the participants in the UK Biobank and HCP studies for their contribution to open science.

Author roles
MA, SLH, and DF conceptualized the study and methods. MA, PZ, and MM ran the data cleaning and analysis of the UK Biobank portion of the study. MA, SH, and GG ran the data cleaning and analysis of the HCP portion of the study. MA, SH, and DF wrote the paper.

Funding

This study was supported via the generous contribution of grants for DF from The Koerner Family Foundation New Scientist Program, The Krembil Foundation, the Canadian Institutes of Health Research, and the CAMH Discovery Fund. Author MA was further supported by the CAMH womenmind postdoctoral fellowship.

Data and Code Availability

UK Biobank data is available through an application for access process. More information about it is available through this URL: https://www.ukbiobank.ac.uk/enable-your-research/apply-for-access. HCP Young Adult data is freely available through this URL: https://www.humanconnectome.org/study/hcp-young-adult/data-releases.
Codes to analyze this data are currently being organized for sharing and will be available on Github.

References

1. Waskom, M.L. *J. Open Source Softw.* **6**, 3021 (2021).
2. Miller, K.L. et al. *Nat. Neurosci.* **19**, 1523–1536 (2016).
3. Alfaro-Almagro, F. et al. *NeuroImage* **166**, 400–424 (2018).
4. Wainberg, M. et al. *PLOS Med.* **18**, e1003782 (2021).
5. Jaeger, J. *J. Clin. Psychopharmacol.* **38**, 513–519 (2018).
6. Kroenke, K., Spitzer, R.L. & Williams, J.B.W. *Med. Care* **41**, 1284–1292 (2003).
7. Glasser, M.F. et al. *Nature* **536**, 171–178 (2016).
8. Fischl, B. *NeuroImage* **62**, 774–781 (2012).
9. Hariri, A.R., Tessitore, A., Mattay, V.S., Fera, F. & Weinberger, D.R. *NeuroImage* **17**, 317–323 (2002).
10. Barch, D.M. et al. *NeuroImage* **80**, 169–189 (2013).
11. Haxby, J.V. et al. *Science* **293**, 2425–2430 (2001).
12. Kamitani, Y. & Tong, F. *Nat. Neurosci.* **8**, 679–685 (2005).
13. Kriegeskorte, N., Mur, M. & Bandettini, P. *Front. Syst. Neurosci.* **2**, (2008).
14. Jenkinson, M., Beckmann, C.F., Behrens, T.E.J., Woolrich, M.W. & Smith, S.M. *NeuroImage* **62**, 782–790 (2012).
15. Van Essen, D.C. et al. *NeuroImage* **62**, 2222–2231 (2012).
16. Glasser, M.F. et al. *NeuroImage* **80**, 105–124 (2013).
17. Buysse, D.J., Reynolds, C.F., Monk, T.H., Berman, S.R. & Kupfer, D.J. *Psychiatry Res.* **28**, 193–213 (1989).
18. Pilkonis, P.A. et al. *Psychiatry Res.* **206**, 88–97 (2013).
19. Arevalo-Rodriguez, I. et al. *Cochrane Database Syst. Rev.* **2021**, CD010783 (2021).